

that in the complex solution. A plot of k_{obsd} versus $[H^+]$ gave a straight line with a zero y-intercept. The values for these rate constants are given in Table III.

A mechanism consistent with these observations is shown in Scheme II. The two equilibria represented by K_a and K_c are rapid and are not seen as distinct steps in the complexation reactions. The formation of the chelated phenanthroline complex is consistent with the orange color of the complex and the first-order $[H^+]$ dependence on the reverse reaction. Similar results have been obtained for the Ti^{3+} and V^{2+} reactions with complex I prior to electron transfer.¹¹

For the mechanism in Scheme II, the experimentally determined value of k_r can be written as follows:

$$k_r = k'_{-1}/K_a K_c \quad (5)$$

Unfortunately, no determinations of K_a or K_c are available; thus evaluation of k'_{-1} is not possible.

The kinetic equilibrium constants for formation of the Ni^{2+} and Co^{2+} complexes with I are 239 and 169 M^{-1} , respectively. These values are not strictly comparable to those for the free ligand, since we are dealing with complexation of a 2+ ion with a 3+ complex. However, the values for this process are expected to be much smaller than those for uncomplexed ligand. No values are available for the phenanthroline-2-carboxamide ligand, but for 2-substituted pyridines containing a carboxyl group, the formation

constants are in the range 10^6 – $10^{10} M^{-1}$ ¹² for complexation with Ni^{2+} whereas, for the complexation of $(NH_3)_5Co(2-NHCOpy)^{2+}$ with Ni^{2+} , the kinetically determined equilibrium constant is only $5.6 \times 10^3 M^{-1}$. Presumably, in the case of the phenanthroline-carboxamide ligand, steric effects and the increased electrostatic repulsion will decrease the formation constants of the pentaammine complex substantially.

Conclusions

The complexation reactions of I, which possesses a pendant phenanthroline with a carbonyl group in the 2-position, occur via the carbonyl oxygen and the adjacent nitrogen on the phenanthroline ring. Subsequent rearrangement reactions may occur which result in a tridentate complex involving the carbonyl oxygen and both phenanthroline nitrogens. The latter behavior has been observed for Fe(II), Ti(III), and V(II). Further work on the substitution and electron-transfer reactions of complex I are in progress.

Acknowledgment. We thank Dr. M. Mlekuz and L. Randall for acquiring the ^{13}C NMR spectra. We also thank the Natural Sciences and Engineering Research Council of Canada for financial support.

Supplementary Material Available: Tables of rate constants for metal ion complexation reactions (3 pages). Ordering information is given on any current masthead page.

(11) Johnson, M.; Balahura, R. Unpublished data.

(12) *Stability Constants of Metal-Ion Complexes*; Special Publication No. 17; Chemical Society: London, 1964; Section II, Organic Ligands.

Contribution from the Department of Chemistry, The University of Chicago, 5735 South Ellis Avenue, Chicago, Illinois 60637, and Department of Chemistry and Biochemistry, University of Delaware, Newark, Delaware 19716

Bimetallic Reactivity. Synthesis, Structure, and Reactivity of Homo- and Heterobimetallic Complexes of a Binucleating Macrocyclic Ligand Containing 6- and 4-Coordination Sites

Cassandra Fraser,[†] Laura Johnston,[†] Arnold L. Rheingold,[‡] Brian S. Haggerty,[‡] Graylon K. Williams,[‡] John Whelan,[†] and B. Bosnich^{*,†}

Received October 11, 1991

A binucleating macrocyclic ligand which embodies 6- and 4-coordinate sites has been prepared. Both homobimetallic and site-specific heterobimetallic complexes of Zn(II), Co(II), and Mn(II) have been isolated and characterized. The dimanganese(II) species reacts with dioxygen to give a mixed-valence compound containing both Mn(II) and Mn(III). All of the manganese-containing complexes are effective catalysts for the oxygenation of styrene using iodosobenzene. Crystal structures of these bimetallic complexes confirm the overall structures but also reveal that the 6-coordinate site has an unsymmetrical arrangement of ligands possibly due to macrocyclic strain. The results from these studies suggest modifications which may result in metal cooperativity in dioxygen uptake and for catalytic epoxidation.

1. Introduction

Numerous multimetallic coordination compounds derived from multinucleating ligands have been prepared.¹ For the most part, the objectives of these investigations were to determine the structure and physical properties and to reproduce the coordination of multimetallic sites of metalloproteins.² Few of these studies were directed at the potentially unique reactivities that these systems might provide. The notable exception is that of dioxygen binding where the redox cooperativity of bimetallic complexes has been demonstrated.³ In all of these cases, however, both metals are involved in binding to the dioxygen molecule. We are aware of only one structurally established synthetic example where the dioxygen molecule binds to a single metal of a bimetallic system and where both metals appear to be involved in the reduction of O_2 .⁴ Similarly, in the case of oxo transfer, the oxo moiety is believed to bind to both metals when bimetallic systems are used.⁵

Table I. Magnetic Moments in μ_B at 25 °C for Complexes Derived from the Ligands (pyral) H_2 and (cyclim) H_2

complex	magn moment, μ_B	
	solid	solution ^a
[Co(pyral)]	4.5	4.5
[Zn(cyclim)CoCl]PF ₆	4.9	4.7
[Co(cyclim)CoCl]PF ₆	6.2	6.7 (6.93) ^b
[Co(cyclim)Co](PF ₆) ₂	6.3	6.2 (6.93)
[Mn(pyral)]	5.7	5.8
[Mn(cyclim)ZnCl]PF ₆	5.6	5.8
[Zn(cyclim)MnCl]PF ₆	6.0	6.1
[Mn(cyclim)MnCl]PF ₆	7.7	8.0 (10.95)
[Mn(cyclim)(μ -Cl)MnCl]PF ₆	7.5	7.8 (9.95)

^a [M(pyral)] complexes were measured in methylene chloride; the bimetallics were measured in acetonitrile.⁶ The magnetic moment values given in parentheses are the spin-only values expected for spin-interacting dimers. For bimetallic complexes all of the magnetic moments are calculated for the dimer.

This paper is the first in a series directed at developing binucleating ligands which fully encapsulate one metal but which allow

[†] The University of Chicago.

[‡] University of Delaware.

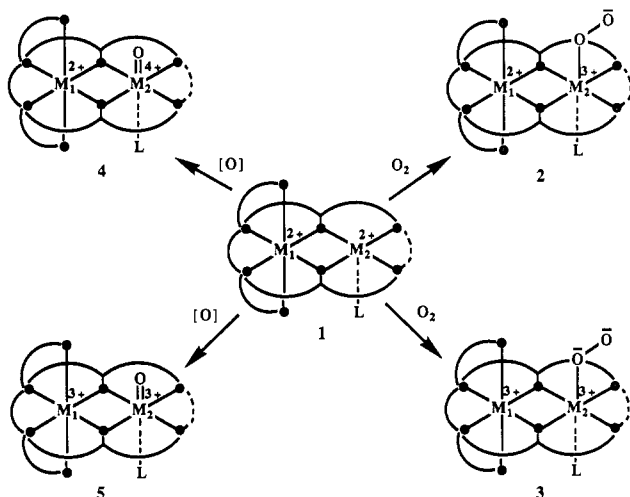


Figure 1. Schematic representation of the bimetallic ligand system incorporating a closed and an open site and the possible reactions with dioxygen and oxo ligands.

the other contiguous metal to bind to reducible substrates. The function of the encapsulated metal is to transfer electrons to the neighboring metal as well as, in some cases, to provide a defined structural framework for selectivity in catalytic reactions. This structural framework for binucleating ligands is distinctive and could provide unique reactivity patterns not always available to the conventional binucleating ligands. The basic structural framework we envision is illustrated in 1. Structure 1 has one metal (M_1) coordinatively saturated in a sexadentate site whereas the other metal (M_2) is either in a square-planar or square-pyramidal site, allowing the substrate to bind at this latter metal. The structure can be macrocyclic or otherwise. In order to il-

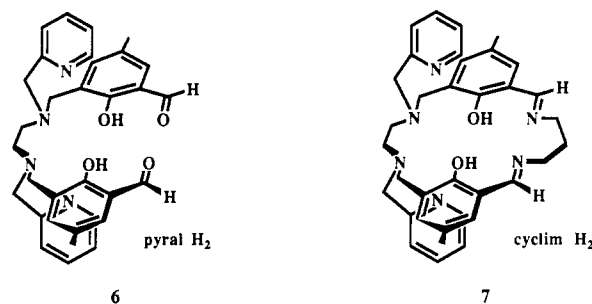
lustrate the potential of structure 1, we consider the redox possibilities after dioxygen binding or formation of oxo complexes using metals in the II oxidation state as examples (Figure 1).

Interaction of O_2 with the open-site metal (M_2) can lead either to the oxidation of M_2 only and the formation of a superoxide 2 or the oxidation of both metals to form a peroxide ligand 3. With appropriate metal combinations it may be possible to induce 4-electron reduction of dioxygen to obtain oxo complexes. These oxo complexes can also be obtained by oxo transfer reagents to form the two possible complexes 4 and 5. Such bimetallic complexes may have distinct reactivity patterns compared to those of monometallic analogues. Further, the sexadentate structure about the closed site can induce chiral discrimination of reactions occurring at the open site. Thus, even with a redox-passive metal in the closed site, the topology illustrated in 1 may provide a new structural concept for asymmetric catalysis.

These are some of the long-term goals which have prompted us to investigate bimetallic systems of this type, but this paper is directed at a number of more immediate questions. These are as follows. What combination of donor atoms is required to obtain oxidation of both metals? This question, of course, depends on which metals we choose. What conditions are required to prepare site-specific heterobimetallic systems without scrambling of the sites? Structure 1 requires that the bridging ligand-metal assembly lie roughly in one plane, and we will investigate which particular ligand features ensure that this be so. There are other subsidiary questions which will be addressed later.

2. Bimetallic Ligand

The two ligands investigated here are 6 and 7. The following considerations went into the design of these ligands. With respect



to the octahedral closed site, it is required that the two pyridyl groups occupy trans, apical positions with respect to the mean molecular bimetallic plane. This is expected because the bis-(pyridyl)ethylenediamine part of the sexadentate chelate consists of three consecutive 5-membered chelate rings. Such quadridentates tend to prefer the cis- α topology.⁶ The other part of the sexadentate ligand, namely, the O-N-N-O donor atom sequence, consists of a succession of 6-, 5-, and 6-membered chelate rings. This ring sequence usually prefers a planar arrangement⁶ as required. Thus, other things being equal, this confluence of chelate rings should give the desired stereochemistry. Although generally reliable for monometallic systems, these arguments are yet to be tested for bimetallic complexes.

The open site of 7 resembles the coordination of salen complexes. The salen complexes of Co(II)⁷ and Mn(II)⁸ are known

- (1) (a) Vigato, P. A.; Tamburini, S.; Fenton, D. E. *Coord. Chem. Rev.* **1990**, *106*, 25. (b) Groh, S. E. *Isr. J. Chem.* **1976**, *15*, 277. (c) Fenton, D. E. In *Advances in Inorganic and Bioinorganic Mechanisms*; Sykes, A. G., Ed.; Academic Press: London, 1983; Vol. II, p 187. (d) Martell, A. E.; Sawyer, D. T., Eds. *Oxygen Complexes and Oxygen Activation by Transition Metals*; Plenum Press: New York, 1988. (e) Glick, M. D.; Lintvedt, R. L. *Prog. Inorg. Chem.* **1976**, *21*, 233. (f) Casellato, U.; Vigato, P. A. *Coord. Chem. Rev.* **1977**, *23*, 31. (g) Casellato, U.; Vigato, P. A.; Fenton, D. E.; Vidali, M. *Chem. Soc. Rev.* **1979**, *8*, 199. (h) Fenton, D. E.; Casellato, U.; Vigato, P. A.; Vidali, M. *Inorg. Chim. Acta* **1982**, *62*, 57. (i) Fenton, D. E.; Tate, J. R.; Casellato, U.; Tamburini, S.; Vigato, P. A.; Vidali, M. *Inorg. Chim. Acta* **1984**, *83*, 23. (j) Chaudhuri, P.; Wieghardt, K. *Prog. Inorg. Chem.* **1987**, *35*, 329. (k) Wieghardt, K.; Bossek, U.; Bonvoisin, J.; Beauvillain, P.; Girerd, J.-J.; Nuber, B.; Weiss, J.; Heinze, J. *Angew. Chem., Int. Ed. Engl.* **1986**, *25*, 1030. (l) Wieghardt, K.; Bossek, U.; Ventur, D.; Weiss, J. *J. Chem. Soc., Chem. Commun.* **1985**, 347. (m) Sheats, J. E.; Czernuszewicz, R. S.; Dismukes, G. C.; Rheingold, A. L.; Petrouleas, V.; Stubbe, J.; Armstrong, W. H.; Beer, R. H.; Lippard, S. J. *J. Am. Chem. Soc.* **1987**, *109*, 1435. (n) Bossek, U.; Weyhermüller, T.; Wieghardt, K.; Nuber, B.; Weiss, J. *J. Am. Chem. Soc.* **1990**, *112*, 6387. (o) Mathur, P.; Crowder, M.; Dismukes, G. C. *J. Am. Chem. Soc.* **1987**, *109*, 5227. (p) Wieghardt, K. *Angew. Chem., Int. Ed. Engl.* **1989**, *28*, 1153. (q) Brudvig, G. W.; Crabtree, R. H. *Prog. Inorg. Chem.* **1989**, *37*, 99. (r) Coleman, W. M.; Taylor, L. T. *Coord. Chem. Rev.* **1980**, *32*, 1. (s) Lawrence, G. D.; Sawyer, D. T. *Coord. Chem. Rev.* **1978**, *27*, 173. (t) Christou, G. *Acc. Chem. Res.* **1989**, *22*, 328.
- (2) (a) Karlin, K. D.; Gultne, Y. *Prog. Inorg. Chem.* **1987**, *35*, 219. (b) Sorrell, T. N. *Tetrahedron* **1989**, *45*, 3. (c) Karlin, K. D.; Zubietta, J., Eds. *Cooper Coordination Chemistry: Biochemical & Inorganic Perspectives*; Adenine Press: New York, 1983. (d) Gamp, H.; Zuberbühler, A. D. In *Metal Ions in Biological Systems*; Sigel, H., Ed.; Marcel Dekker, Inc.: New York, 1987; Vol. 12, p 113. (e) Zuberbühler, A. D. In *Metal Ions in Biological Systems*; Sigel, H., Ed.; Marcel Dekker, Inc.: New York, 1976; Vol. 5, p 325. (f) Suzuki, M.; Kanatomi, H.; Murase, I. *Chem. Lett.* **1981**, 1745. (g) Suzuki, M.; Ueda, I.; Kanatomi, H.; Murase, I. *Chem. Lett.* **1983**, 185.
- (3) Halpern, J.; Goodall, B. L.; Khare, G. P.; Lim, H. S.; Pluth, J. J. *J. Am. Chem. Soc.* **1975**, *97*, 2301.
- (4) (a) Fantai, A.; Margerum, L. D.; Valentine, J. S. *J. Am. Chem. Soc.* **1986**, *108*, 5006. (b) Murch, B. P.; Bradley, F. C.; Que, L., Jr. *J. Am. Chem. Soc.* **1986**, *108*, 5027. (c) Kitajima, N.; Fukui, H.; Morooka, Y. *J. Chem. Soc., Chem. Commun.* **1988**, 485. (d) Vincent, J. B.; Huffman, J. C.; Christou, G.; Li, Q.; Nanny, M. A.; Hendrickson, D. N.; Fong, R. H.; Fish, R. H. *J. Am. Chem. Soc.* **1988**, *110*, 6898.

- (5) (a) Bosnich, B.; Gillard, R. D.; McKenzie, E. D.; Webb, G. A. *J. Chem. Soc. A* **1966**, 1331. (b) Bosnich, B.; MacB. Harrowfield, J.; Boucher, H. *Inorg. Chem.* **1975**, *14*, 815. (c) Buckingham, D. A.; Marzilli, P. A.; Sargeson, A. M. *Inorg. Chem.* **1967**, *6*, 1032. (d) Hamilton, H. D.; Alexander, M. G. *J. Am. Chem. Soc.* **1967**, *89*, 5065.

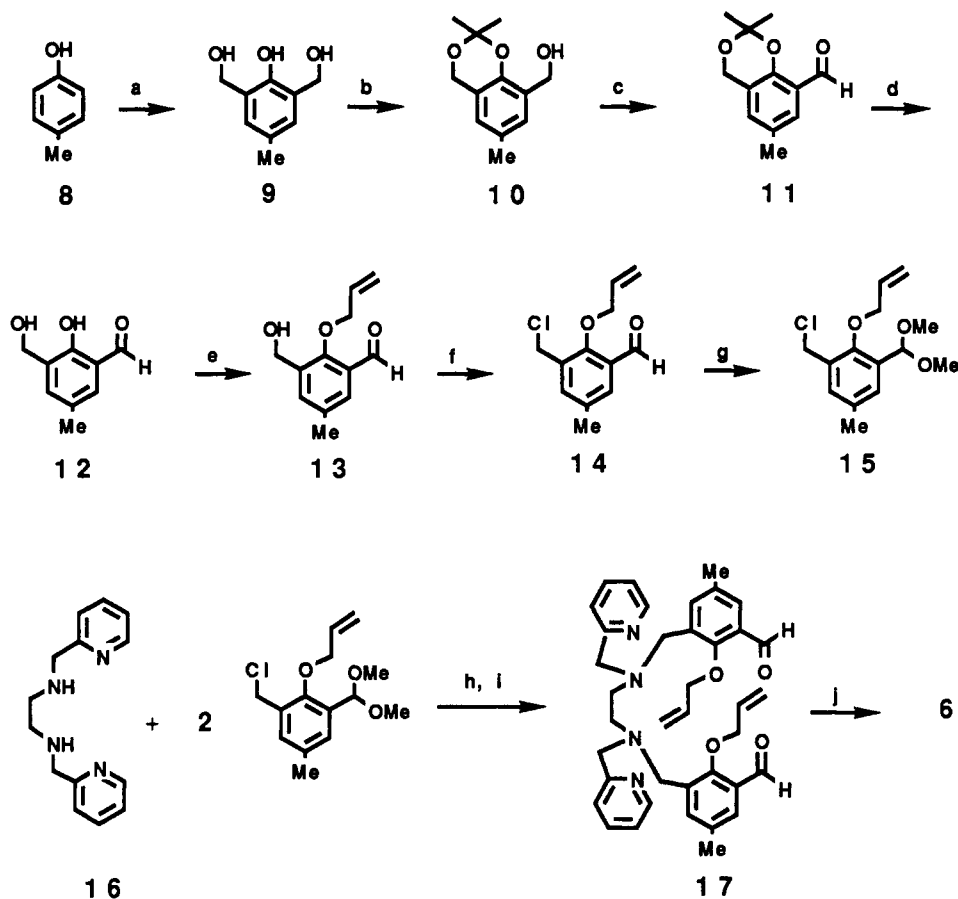


Figure 2. Outline of the synthesis of ligand 6.

to take up dioxygen, and the manganese Schiff base complexes are useful oxo transfer catalysts.⁹

3. Ligand Synthesis

An outline of the synthesis of **6** is shown in Figure 2. Although each step proceeds cleanly in high yield and a synthetic run can produce gram quantities of the ligand, the procedure is cumbersome. The triol **9** is prepared by a modification of Ullman's procedure¹⁰ and the equivalent sites of **9** are differentiated by the acetonide **10**. Although Swern oxidation¹¹ of **10** generated the aldehyde **11** in excellent yield, it was limited in scale, and it was convenient for large-scale preparations to oxidize **10** with NaOCl by phase-transfer catalysis.¹² Deprotection of **11** followed by selective phase-transfer-catalyzed phenolic allylation gave **13** which

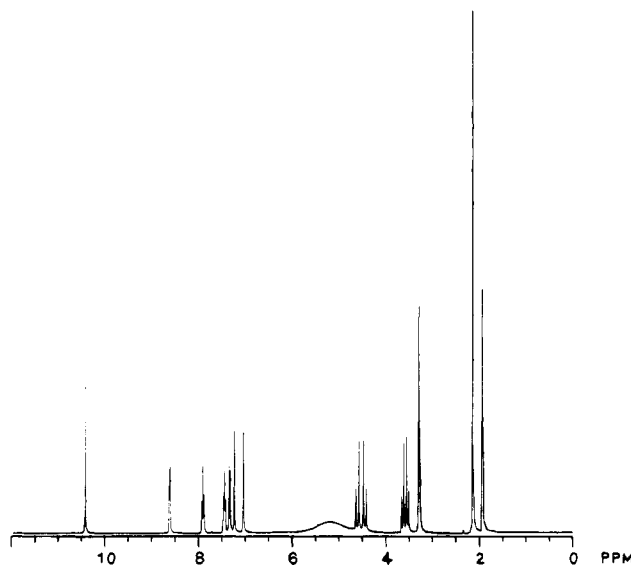


Figure 3. ^1H NMR spectrum of $[\text{Co}(\text{pyral})]^+$ in deuterated acetonitrile solution. It will be noted that only one set of signals is observed for each type of proton.

was chlorinated under mild conditions and then protected to give **15**. Coupling of **15** with **16** gave **17** after acidic workup. The allyl protecting groups were removed by the use of a catalytic amount of $[\text{Pd}(\text{PPh}_3)_4]$ and sodium dimethylmalonate under mild

- (7) (a) Niederhoffer, E. C.; Timmons, J. H.; Martell, A. E. *Chem. Rev.* **1984**, *84*, 137. (b) Jones, R. D.; Summerville, D. A.; Basolo, F. *Chem. Rev.* **1979**, *79*, 139.
- (8) (a) Larson, E. J.; Pecoraro, V. L. *J. Am. Chem. Soc.* **1991**, *113*, 3810. (b) Matsushita, T.; Yarinio, T.; Masuda, I.; Shono, T.; Shinra, K. *Bull. Chem. Soc. Jpn.* **1973**, *46*, 1712. (c) Yarinio, T.; Matsushita, T.; Masuda, I.; Shinra, K. *Chem. Commun.* **1970**, 1317. (d) Lewis, J.; Mabbs, F. E.; Weigold, H. *J. Chem. Soc. A* **1968**, 1699.
- (9) (a) Srinivasan, K.; Michael, P.; Kochi, J. K. *J. Am. Chem. Soc.* **1986**, *108*, 2309. (b) Zhang, W.; Loebach, J. L.; Wilson, S. R.; Jacobsen, E. N. *J. Am. Chem. Soc.* **1990**, *112*, 2801. (c) Zhang, W.; Jacobsen, E. N. *J. Org. Chem.* **1991**, *56*, 2296.
- (10) (a) Ullmann, F.; Brittner, K. *Chem. Ber.* **1909**, *42*, 2539. (b) Gagne, R. R.; Spiro, C. L.; Smith, T. J.; Hamann, C. A.; Thies, W. R.; Shiemke, A. K. *J. Am. Chem. Soc.* **1981**, *103*, 4073.
- (11) Mancuso, A. J.; Swern, D. *Synthesis* **1981**, 165.
- (12) Lee, G. A.; Freedman, H. H. *Tetrahedron Lett.* **1976**, *20*, 1641.

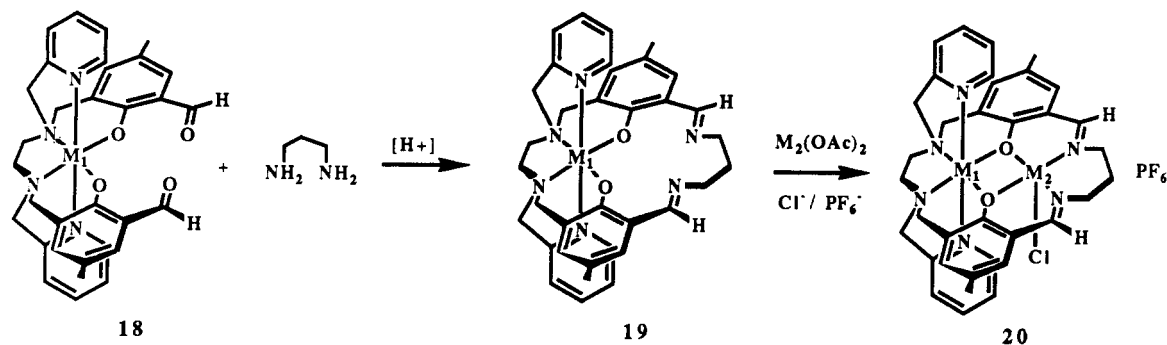
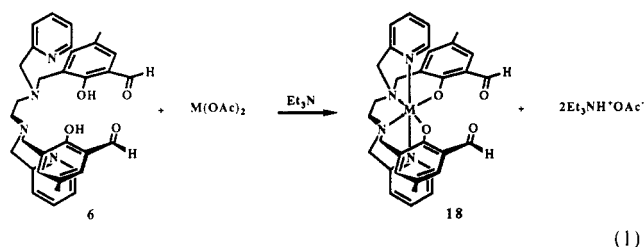


Figure 4. Outline of the procedure generating heterobimetallic cyclim complexes.

conditions.¹³ The product **6** was a viscous oil which could be purified as its solid Zn(II) complex and could be freed of the metal by H₂S. The ligand **6** was stored as its zinc complex.

4. Synthesis of Complexes

The mononuclear complexes of the dialdehyde ligand **6** are readily prepared by allowing **6** to react with the metal acetate and triethylamine in alcohol solvents (eq 1). In this way the



generally insoluble complexes of Zn(II), Co(II), and Mn(II) were prepared, and oxidation of the Co(II) complex with [FeCp₂]PF₆ gave the Co(III) species. The diamagnetic Zn(II) and Co(III) complexes showed ¹H NMR spectra which confirmed that the compounds possess a 2-fold rotation axis, supporting the prediction that the mononuclear complexes have the structure **18**. The ¹H NMR of the Co(III) complex is shown in Figure 3.

Given the rigid structure of **18** which fixes the orientation of the two aldehyde groups, we expected that **18** would condense with diamines to give the desired macrocyclic species. This proved to be the case but the results were dependent on the span of the diamine. Thus addition of 2 equiv of M(OAc)₂ to **6** followed by reaction with either ethylenediamine or *o*-phenylenediamine yielded intractable products presumably because these diamines cannot easily span the two aldehyde centers. A similar observation has been made before for analogous compounds.¹⁴ Expanding the ring size with 1,3-diaminopropane led to macrocyclic condensation in excellent yields.

The homobimetallic complexes are thus readily prepared by first adding 2 equiv of M(OAc)₂ to the dialdehyde **6** in ethanol solution and then slowly adding 1,3-diaminopropane. After reflux for several hours addition of NH₄PF₆ gave crystalline products. However, many of these (PF₆)₂ salts gave analytical data which indicated that the products cocrystallized with varying amounts of solvent of crystallization. Analytically pure samples were obtained by addition of chloride ions to give the monochloro species of the type [M(cyclim)MCl]PF₆. (The convention we adopt here is to designate the bimetallic complexes by the following sequence: closed-site metal, binucleating ligands, and open-site metal, followed by any ligands bound to the open-site metal.)

Despite the expectation that the metal in the closed site would be both kinetically and thermodynamically stable during incorporation of the open-site metal, attempts to prepare heterobimetallic species by sequential addition of metal salts followed by

the cyclization procedure adopted for the preparation of the homobimetallic complexes led to extensive scrambling. In order to obtain site-specific heterobimetallic complexes, a new milder procedure was adopted. This is outlined in Figure 4. The monometallic dialdehyde complex **18** was cyclized with 1,3-diaminopropane under acid catalysis, and then the second metal was added. Under these conditions heterobimetallic compounds were obtained which had the correct 1:1 ratio of the two metals and for which the electronic spectra suggested that the metals were in the expected sites. We should note, however, that simply determining that a 1:1 ratio of metals is present in a heterobimetallic system does not establish that no site interchange has occurred. Given the mild synthetic conditions employed and the consistency of the physical data, it seems highly probable that the heterobimetallic complexes described here are site-specific within at least a few percent.

5. Physical Characterization

Molar conductances of complexes of the type [M₁(cyclim)M₂](PF₆)₂ in acetonitrile solutions were in the range 276–290 Ω⁻¹ cm² mol⁻¹ consistent with 2:1 electrolytes¹⁵ whereas the [M₁(cyclim)M₂Cl]PF₆ species were 1:1 electrolytes in acetonitrile solutions (122–134 Ω⁻¹ cm² mol⁻¹), indicating that the chloro ligand was bound to the open-site metal.

Magnetic moments were measured for the samples both as powdered solids and in solution.¹⁶ The results are presented in Table I. The solid and solution moments correlate reasonably well. A comparison of the zinc-containing complexes with species containing two magnetically active metals gives an indication of the degree of magnetic coupling.¹⁴ Thus, for example, a comparison of the moments observed for [Mn(cyclim)ZnCl]PF₆, [Zn(cyclim)MnCl]PF₆ and [Mn(cyclim)MnCl]PF₆ indicates that magnetic coupling occurs in the last complex. Similar observations obtain for the Co(II) species. The magnetic moments for the Co(II) and Mn(II) complexes indicate that the metals exist in the expected high-spin configurations.^{17,18} The last entry in Table I is a Mn(II)–Mn(III) complex, the provenance and structure of which we discuss presently.

The electronic absorption spectra of all complexes are characterized by a strong ligand absorption at around 365 nm, which tails into the visible region and tends to obscure contiguous weaker d–d transitions. As expected, the spin-free Mn(II) complexes show no detectable d–d transitions. The Co(II) complexes, however, show a multiplicity of d–d transitions which extend into the near-IR region. We show the spectra of [Co(pyr)]⁺, [Zn(cyclim)CoCl]⁺, and [Co(cyclim)CoCl]⁺ in Figure 5. It will be noted that spectra of the last two complexes are remarkably similar. When these spectra are compared to that of the octahedral species

(13) (a) Takahashi, K.; Miyaki, A.; Hata, G. *Bull. Chem. Soc. Jpn.* **1972**, *45*, 230. (b) Hata, G.; Takahashi, K.; Miyaki, A. *Chem. Commun.* **1970**, 1392. (c) Hey, H.; Arpe, H.-J. *Angew. Chem., Int. Ed. Engl.* **1973**, *12*, 928.

(14) Pilkington, N. H.; Robson, R. *Aust. J. Chem.* **1970**, *23*, 2225.

(15) (a) Geary, W. J. *Coord. Chem. Rev.* **1971**, *7*, 107. (b) Walton, R. A. *Q. Rev., Chem. Soc.* **1965**, *19*, 126.

(16) (a) Evans, D. F. *J. Chem. Soc.* **1959**, 2003. (b) Live, D. H.; Chan, S. I. *Anal. Chem.* **1970**, *42*, 791.

(17) (a) Banci, L.; Bencini, A.; Benelli, C.; Gatteschi, D.; Zanchini, C. *Struct. Bonding (Berlin)* **1982**, *52*, 52. (b) Suzuki, M.; Kanatomi, H.; Murase, I. *Bull. Chem. Soc. Jpn.* **1984**, *57*, 36.

(18) Chiswell, B.; McKenzie, E. D.; Lindoy, L. F. In *Comprehensive Coordination Chemistry*; Wilkinson, G., Ed.; Pergamon Press: New York, **1987**, Vol. 4, Chapter 41.

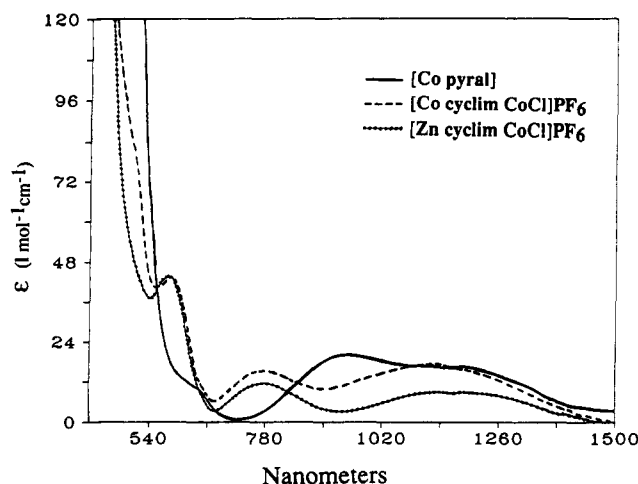


Figure 5. Visible and near-infrared spectra of the compounds indicated. The [Co(pyral)] complex was measured in methylene chloride; the other two were run in acetonitrile solutions.

[Co(pyral)], the only absorption that can be assigned uniquely to the open 5-coordinate site is the one at around 760 nm. Absorptions in this region have been ascribed as characteristic of square-pyramidal spin-free Co(II) complexes.¹⁹ The other absorptions have positions and intensities normally expected of octahedral and square-pyramidal spin-free Co(II) complexes.^{17,20}

Cyclic voltammetry of the bimetallic complexes in acetonitrile solutions gave no waves indicating reversible oxidation, and the method was not found to be useful in characterizing the complexes.

6. Reactivity

The oxidative reactivity of the bimetallic complexes revealed a number of interesting features. All of the complexes were inert to O₂ in the solid state but displayed variable reactivity in acetonitrile solution. Exposure of [Zn(cyclim)MnCl]⁺ and [Mn(cyclim)MnCl]⁺ to air in acetonitrile caused the yellow solutions to turn brown, the latter complex reacting faster. After air was bubbled through the solution for 24 h, the mixed-valence complex [Mn(cyclim)(μ-Cl)MnCl]PF₆ was isolated as brown-black crystals from the dimanganese(II) precursor. As we show in the next section, the mixed-valence complex contains a Mn(III) in the open site and the Mn(II) is retained in the closed site. The [Zn(cyclim)MnCl]⁺ species gives a brown powder which consists of the starting material and probably MnO₂. The same Mn(II)/Mn(III) complex can be prepared by the addition of [FeCp₂]⁺ in the presence of Cl⁻ ions. Attempts to prepare a Mn(III)/Mn(III) species by the addition of amounts in excess of 2 equiv of [FeCp₂]⁺ yielded the same Mn(II)/Mn(III) product, suggesting that the oxidation of the closed-site Mn(II) is more difficult after the Mn(II) in the open site has been oxidized. Addition of varying equivalents of [FeCp₂]⁺ to solutions of [Zn(cyclim)MnCl]⁺ led to the same products as were observed for the reaction with O₂.

The Co(II) complexes were not readily oxidized by O₂. The [Zn(cyclim)CoCl]⁺ and [Co(cyclim)CoCl]⁺ species were essentially inert to O₂ in acetonitrile solutions. Under similar conditions, the [Co(cyclim)Co]²⁺ complex slowly darkened over several days but no clean products could be isolated. Attempts to oxidize dicobalt(II) complexes with stronger one- and two-electron oxidizing agents such as NO and NO⁺ gave dramatic color changes, but the products were unstable and could not be isolated in pure form. It thus appears that cobalt(III) bimetallic species with the present set of ligands are unstable.

The ability of these bimetallic complexes to act as epoxidation catalysts was tested using iodosobenzene as a cocatalyst and styrene as a substrate. Some of the results are collected in Table

Table II. Epoxidation of Styrene Using Bimetallic Catalysts^a and Iodosobenzene^b in CH₃CN at 25 °C

catalyst	% products ^c		turnover, ^d freq, h ⁻¹	% react ^e
	Ph epoxide	Ph aldehyde		
[Zn(cyclim)Zn] ²⁺	0	0	0	0
[Co(cyclim)CoCl] ⁺	4	<1	<1	9
[Zn(cyclim)MnCl] ⁺	39	11	20	76
[Mn(cyclim)ZnCl] ⁺	35	6	20	65
[Mn(cyclim)MnCl] ⁺	66	23	61	89
[Mn(cyclim)(μ-Cl)MnCl] ⁺	68	23	183	91
[Mn(saltn)]	12	<1	5	31

^a 1 mol % catalyst. ^b 2 equiv of iodosobenzene to substrate. ^c Product percentages after 2 h based on styrene submitted. ^d Turnover frequency = number of moles of substrate turnover per mole of catalyst per hour for initial rate. ^e % reaction = % product produced after catalysis ceases.

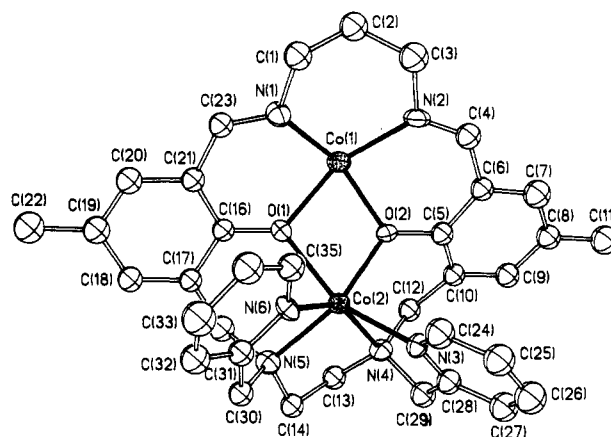


Figure 6. ORTEP drawing and labeling scheme for [Co(cyclim)Co]²⁺ (cation of 1). Ellipsoids are at 30% probability. Hydrogens are omitted for clarity.

II. The [Mn(saltn)] complex is included for comparison (tn = 1,3-diaminopropane).

As expected the dizinc complex is not a catalyst for epoxidation and the dicobalt species shows marginal catalytic activity. The manganese species, however, are effective catalysts. We note that the open-site manganese species, [Zn(cyclim)MnCl]⁺, and the corresponding complex with the closed-site manganese, [Mn(cyclim)ZnCl]⁺, show similar catalytic activity although the ratios of epoxide to aldehyde are different. This result suggests that the manganese in the sexadentate site dissociates one of the pyridyl ligands to open a site for forming the catalytically active oxo species. Whether this occurs with the dimanganese catalysts is not known, but it is clearly possible. The dimanganese species are the most effective catalysts. The two dimanganese complexes lead essentially to the same product ratios, and both catalysts consume ~90% of the substrate. It seems probable, therefore, that the same catalytically active intermediate is being generated from the two dimanganese catalytic precursors. The fact that the mixed-valence dimanganese complex has a much faster initial rate may reflect the greater ease of attaining the catalytically active species for the mixed-valent catalyst precursor. At the midpoint of reaction both catalysts have similar rates. All of the catalysts become ineffective after a varying number of turnovers, which is probably associated with the destruction of the ligand. A comparison of the catalysis using [Mn(saltn)] with the two dimanganese complexes⁹ indicates that the bimetallic systems produce catalysts which have greater turnover numbers, different product ratios, and faster rates. Whether this is simply due to the presence of two manganese atoms per mole of catalyst acting essentially independently or due to cooperative behavior is not resolved by these experiments.

7. Structures

Single-crystal X-ray diffraction structures of the following bimetallic complexes, [Mn(cyclim)MnCl]PF₆ (4), [Co(cyclim)-

- (19) (a) Lions, F.; Dance, I. G.; Lewis, J. J. *Chem. Soc. A* 1967, 565. (b) Hoskins, B. F.; Robson, R.; Williams, G. A. *Inorg. Chim. Acta* 1976, 16, 121.
(20) Lever, A. B. P. *Inorganic Electronic Spectroscopy*, 2nd ed.; Elsevier: New York, 1984; pp 480-494.

Table III. Crystal, Data Collection and Refinement Parameters for 1-4

	1	2	3	4
(a) Crystal Parameters				
formula	C ₃₅ H ₃₅ N ₆ O ₂ P ₂ F ₁₂ Co ₂ ·2CH ₃ CN	C ₃₅ H ₃₈ N ₆ O ₂ Cl ₂ PF ₆ Mn ₂ ·CH ₃ CN	C ₃₅ H ₃₈ N ₆ O ₂ PF ₆ ClCo ₂	C ₃₅ H ₃₈ N ₆ O ₂ ClPF ₆ Mn ₂
fw	1064.60	941.51	873.01	865.02
cryst syst	orthorhombic	monoclinic	monoclinic	monoclinic
space group	<i>Pbca</i>	<i>P2₁</i>	<i>P2₁/n</i>	<i>P2₁/n</i>
<i>a</i> , Å	15.118 (6)	11.329 (2)	10.296 (2)	10.310 (2)
<i>b</i> , Å	28.528 (9)	14.228 (3)	16.835 (3)	17.068 (3)
<i>c</i> , Å	20.920 (6)	12.745 (2)	21.923 (4)	21.874 (4)
β, deg		92.29 (2)	97.38 (1)	96.84 (1)
<i>V</i> , Å ³	9022 (6)	2052.6 (7)	3768.2 (13)	3821.9 (13)
<i>Z</i>	8	2	4	4
cryst dims, mm	0.21 × 0.30 × 0.42	0.30 × 0.30 × 0.48	0.21 × 0.21 × 0.38	0.30 × 0.40 × 0.42
cryst color	dark red	dark brown	dark brown-green	yellow
<i>D</i> (calc), g cm ⁻³	1.568	1.523	1.538	1.503
μ(Mo Kα), cm ⁻¹	8.84	7.63	10.60	8.25
temp, K	297	297	297	298
(b) Data Collection				
diffractometer	Nicolet R3m			
monochromator	graphite			
radiation	Mo Kα (λ = 0.71073 Å)			
2θ scan range, deg	4-45	4-46	4-48	4-48
data colld (<i>h,k,l</i>)	+17,+31,+23	±13,±16,+15	±12,+19,+25	±12,+20,+20
no. of reflns colctd	6517	5963	5634	6416
no. of indept reflns	5897	5949	5254	6007
no. of indept obsd reflns	2748	4154	2934	3644
<i>F_o</i> ≥ <i>nσ</i> (<i>F_o</i>) (<i>n</i> = 5)				
std reflns	3 std/197 reflns	3 std/197 reflns	3 std/197 reflns	3 std/197 reflns
var in stds	~2	<1	~3	<2
(c) Refinement				
<i>R</i> (<i>F</i>), %	8.60	6.18	5.51	5.12
<i>Rw</i> (<i>F</i>), %	9.13	6.40	5.76	5.41
Δ/ <i>σ</i> (max)	0.040	0.050	0.120	0.014
Δ(ρ), e Å ⁻³	1.239	0.723	0.551	0.527
<i>N_o</i> / <i>N_v</i>	7.3	8.3	6.2	7.6
GOF	1.632	1.111	1.045	1.198

Table VIII. Selected Bond Distances and Angles for [Co(cyclim)Co](PF₆)₂ (1)

Bond Distances (Å)			
Co(1)-O(1)	2.037 (9)	Co(1)-O(2)	1.962 (8)
Co(1)-N(1)	2.030 (11)	Co(1)-N(2)	2.070 (11)
Co(2)-O(1)	2.126 (9)	Co(2)-O(2)	2.008 (8)
Co(2)-N(3)	2.148 (10)	Co(2)-N(4)	2.219 (10)
Co(2)-N(5)	2.153 (11)	Co(2)-N(6)	2.144 (10)
O(1)-C(16)	1.318 (15)	O(2)-C(5)	1.355 (15)
Bond Angles (deg)			
Co(1)-O(1)-Co(2)	99.4 (4)	Co(1)-O(2)-Co(2)	106.2 (4)
O(1)-Co(1)-O(2)	74.0 (3)	O(1)-Co(1)-N(1)	89.7 (4)
O(2)-Co(1)-N(1)	149.9 (4)	O(1)-Co(1)-N(2)	155.5 (4)
O(2)-Co(1)-N(2)	88.2 (4)	N(1)-Co(1)-N(2)	98.1 (4)
O(1)-Co(2)-O(2)	71.2 (3)	O(1)-Co(2)-N(3)	151.9 (4)
O(2)-Co(2)-N(3)	91.1 (4)	O(1)-Co(2)-N(4)	122.4 (4)
O(2)-Co(2)-N(4)	87.3 (3)	N(3)-Co(2)-N(4)	76.7 (4)
O(1)-Co(2)-N(5)	88.7 (4)	O(2)-Co(2)-N(5)	146.9 (4)
N(3)-Co(2)-N(5)	116.1 (4)	N(4)-Co(2)-N(5)	81.6 (4)
O(1)-Co(2)-N(6)	81.8 (4)	O(2)-Co(2)-N(6)	122.5 (4)
N(3)-Co(2)-N(6)	90.4 (4)	N(4)-Co(2)-N(6)	148.0 (4)
N(5)-Co(2)-N(6)	78.1 (4)	Co(1)-O(1)-C(16)	127.8 (8)
Co(1)-O(2)-C(5)	126.4 (8)	Co(2)-O(1)-C(16)	125.6 (8)
Co(2)-O(2)-C(5)	126.7 (8)		

CoCl]PF₆ (3), [Co(cyclim)Co](PF₆)₂ (1), and [Mn(cyclim)(μ-Cl)MnCl]PF₆ (2) were determined (Tables III-XI). These structures are shown in Figures 6-9. Although the monomeric species [Zn(pyr)] and [Co(pyr)]⁺ have a C₂ symmetrical arrangement of the chelate arms, all of the bimetallic macrocyclic systems have an unsymmetrical arrangement of ligands at the closed site where both pyridyl ligands lie on the same side of the mean molecular plane. It all of the structures the closed site resembles a trigonal-prismatic structure, whereas the open site is square pyramidal or square planar. In the case of the mixed-valence structure [Mn(cyclim)(μ-Cl)MnCl]PF₆, the Mn^{III} in the open site is octahedral and the closed site resembles a trigonal-prismatic geometry having one disconnected phenolic bridging

Table IX. Selected Bond Distances and Angles for [Mn(cyclim)(μ-Cl)MnCl](PF₆) (2)

Bond Distances (Å)			
Mn(1)-Cl(1)	2.422 (3)	Mn(1)-Cl(2)	2.780 (3)
Mn(1)-O(1)	1.879 (6)	Mn(1)-O(2)	1.902 (6)
Mn(1)-N(1)	2.040 (8)	Mn(1)-N(2)	2.013 (8)
Mn(2)-Cl(2)	2.507 (3)	Mn(2)-O(1)	2.261 (5)
Mn(2)-N(3)	2.307 (7)	Mn(2)-N(4)	2.329 (7)
Mn(2)-N(5)	2.389 (7)	Mn(2)-N(6)	2.304 (7)
O(1)-C(16)	1.342 (10)	O(2)-C(5)	1.318 (11)
Bond Angles (deg)			
Cl(1)-Mn(1)-Cl(2)	178.6 (1)	Cl(1)-Mn(1)-O(1)	96.0 (2)
Cl(2)-Mn(1)-O(1)	82.5 (2)	Cl(1)-Mn(1)-O(2)	100.9 (2)
Cl(2)-Mn(1)-O(2)	79.0 (2)	O(1)-Mn(1)-O(2)	79.8 (2)
Cl(1)-Mn(1)-N(1)	91.4 (2)	Cl(2)-Mn(1)-N(1)	88.4 (2)
O(1)-Mn(1)-N(1)	88.5 (3)	O(2)-Mn(1)-N(1)	163.8 (3)
Cl(1)-Mn(1)-N(2)	92.3 (2)	Cl(2)-Mn(1)-N(2)	89.1 (2)
O(1)-Mn(1)-N(2)	169.0 (3)	O(2)-Mn(1)-N(2)	91.6 (3)
N(1)-Mn(1)-N(2)	98.5 (3)	Cl(2)-Mn(2)-O(1)	82.4 (2)
Cl(2)-Mn(2)-N(3)	87.2 (2)	O(1)-Mn(2)-N(3)	164.3 (2)
Cl(2)-Mn(2)-N(4)	122.5 (2)	O(1)-Mn(2)-N(4)	122.8 (2)
N(3)-Mn(2)-N(4)	72.8 (2)	Cl(2)-Mn(2)-N(5)	158.2 (2)
O(1)-Mn(2)-N(5)	79.0 (2)	N(3)-Mn(2)-N(5)	108.2 (2)
N(4)-Mn(2)-N(5)	77.7 (2)	Cl(2)-Mn(2)-N(6)	92.8 (2)
O(1)-Mn(2)-N(6)	82.9 (2)	N(3)-Mn(2)-N(6)	85.8 (3)
N(4)-Mn(2)-N(6)	136.5 (3)	N(5)-Mn(2)-N(6)	73.7 (3)
Mn(1)-Cl(2)-Mn(2)	74.2 (1)	Mn(1)-O(2)-C(5)	130.4 (5)
Mn(1)-O(1)-C(16)	129.5 (5)	Mn(2)-O(1)-C(16)	125.7 (5)

ligand. The [Co(cyclim)CoCl]⁺ and [Mn(cyclim)MnCl]⁺ ions are isostructural. The X-ray parameters and the bond lengths and angles are given in Tables III and VIII-XI and in the supplementary material.

That the unsymmetrical structures are not caused by the presence of a chloro group in the open site is suggested by the fact that the [Co(cyclim)CoCl]⁺ and [Co(cyclim)Co]²⁺ ions have similar unsymmetrical structures. Thus we conclude that there is an inherent structural feature of the binucleating macrocyclic

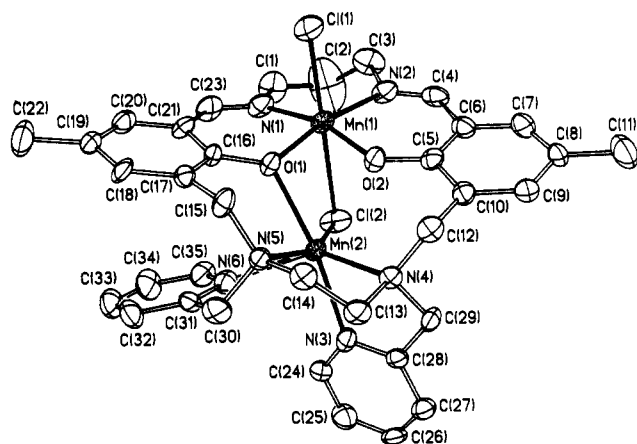


Figure 7. ORTEP drawing and labeling scheme for $[\text{Mn}(\text{cyclim})(\mu\text{-Cl})\text{-MnCl}]^+$ (cation of 2). Ellipsoids are at 30% probability. Hydrogens are omitted for clarity.

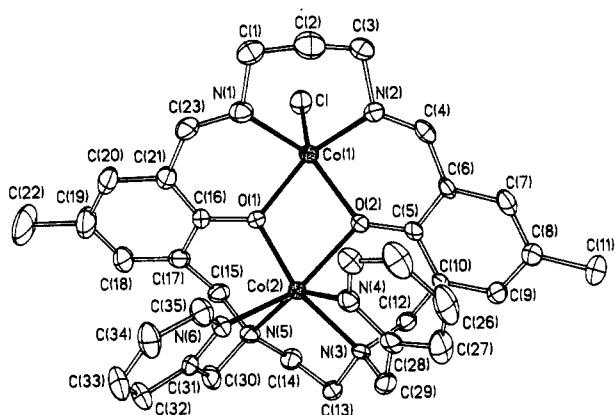


Figure 8. ORTEP drawing and labeling scheme for $[\text{Co}(\text{cyclim})\text{CoCl}]^+$ (cation of 3). Ellipsoids are at 30% probability. Hydrogens are omitted for clarity.

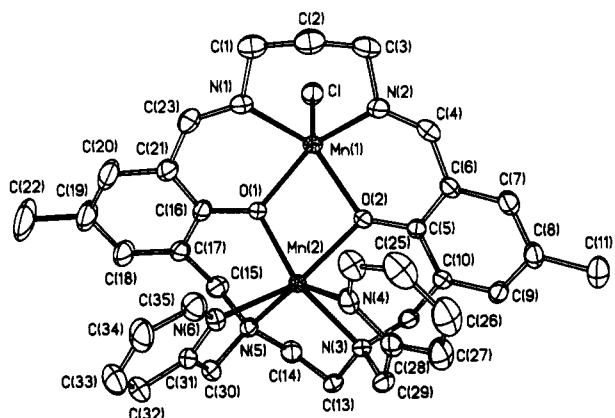


Figure 9. ORTEP drawing and labeling scheme for $[\text{Mn}(\text{cyclim})\text{MnCl}]^+$ (cation of 4). Ellipsoids are at 30% probability. Hydrogens are omitted for clarity.

ligand that causes the asymmetry. As revealed in the structures, the trimethylene diimine link prefers to adopt a (symmetrical) chair conformation. This, in turn, forces the phenolic groups to adopt a conformation where these bridging groups lie on the same side of the mean macrocyclic plane. As a consequence, these transmitted steric imperatives cause both of the pyridyl ligands to dispose themselves to the same side of the mean molecular plane opposite to that of the phenolic groups.

If this analysis is correct, it follows that to obtain a symmetrical closed-site structure where one pyridyl ligand lies above and the other below the mean macrocyclic plane, the bite angles associated with the ethylenediamine and/or trimethylene diimine links are required to be expanded. We are currently exploring 7-membered

Table X. Selected Bond Distances and Angles for $[\text{Co}(\text{cyclim})\text{CoCl}](\text{PF}_6)$ (3)

Bond Distances (Å)			
Co(1)–Cl	2.310 (2)	Co(1)–O(1)	1.993 (5)
Co(1)–O(2)	2.044 (5)	Co(1)–N(1)	2.115 (6)
Co(1)–N(2)	2.049 (7)	Co(2)–O(1)	1.999 (5)
Co(2)–O(2)	2.236 (5)	Co(2)–N(3)	2.186 (6)
Co(2)–N(4)	2.132 (7)	Co(2)–N(5)	2.207 (7)
Co(2)–N(6)	2.182 (6)		
Bond Angles (deg)			
Co(1)–O(1)–Co(2)	108.3 (2)	Co(1)–O(2)–Co(2)	98.1 (2)
Cl–Co(1)–O(1)	109.2 (2)	Cl–Co(1)–O(2)	116.0 (2)
O(1)–Co(1)–O(2)	75.1 (2)	Cl–Co(1)–N(1)	96.3 (2)
O(1)–Co(1)–N(1)	85.4 (2)	O(2)–Co(1)–N(1)	146.2 (2)
Cl–Co(1)–N(2)	102.8 (2)	O(1)–Co(1)–N(2)	147.8 (2)
O(2)–Co(1)–N(2)	88.5 (2)	N(1)–Co(1)–N(2)	94.0 (3)
O(1)–Co(2)–O(2)	70.8 (2)	O(1)–Co(2)–N(3)	145.5 (2)
O(2)–Co(2)–N(3)	86.9 (2)	O(1)–Co(2)–N(4)	123.0 (2)
O(2)–Co(2)–N(4)	84.0 (2)	N(3)–Co(2)–N(4)	78.5 (2)
O(1)–Co(2)–N(5)	89.2 (2)	O(2)–Co(2)–N(5)	122.6 (2)
N(3)–Co(2)–N(5)	80.9 (2)	N(4)–Co(2)–N(5)	145.2 (2)
O(1)–Co(2)–N(6)	93.0 (2)	O(2)–Co(2)–N(6)	153.6 (2)
N(3)–Co(2)–N(6)	116.1 (2)	N(4)–Co(2)–N(6)	88.0 (2)
N(5)–Co(2)–N(6)	76.3 (2)	Co(1)–O(1)–C(16)	128.3 (4)
Co(1)–O(2)–C(5)	130.0 (4)	Co(2)–O(1)–C(16)	121.7 (4)
Co(2)–O(2)–C(5)	118.0 (4)		

Table XI. Selected Bond Distances and Angles for $[\text{Mn}(\text{cyclim})\text{MnCl}](\text{PF}_6)$ (4)

Bond Distances (Å)			
Mn(1)–Cl	2.340 (2)	Mn(1)–O(1)	2.041 (3)
Mn(1)–O(2)	2.119 (3)	Mn(1)–N(1)	2.217 (4)
Mn(1)–N(2)	2.150 (5)	Mn(2)–O(1)	2.067 (3)
Mn(2)–O(2)	2.218 (3)	Mn(2)–N(3)	2.269 (4)
Mn(2)–N(4)	2.217 (5)	Mn(2)–N(5)	2.282 (4)
Mn(2)–N(6)	2.254 (4)	O(1)–C(16)	1.317 (6)
O(2)–C(6)	1.312 (6)		
Bond Angles (deg)			
Mn(1)–O(1)–Mn(2)	107.6 (2)	Mn(1)–O(2)–Mn(2)	99.7 (1)
Cl–Mn(1)–O(1)	111.9 (1)	Cl–Mn(1)–O(2)	119.2 (1)
O(1)–Mn(1)–O(2)	74.2 (1)	Cl–Mn(1)–N(1)	103.3 (1)
O(1)–Mn(1)–N(1)	82.6 (2)	O(2)–Mn(1)–N(1)	136.6 (2)
Cl–Mn(1)–N(2)	108.2 (1)	O(1)–Mn(1)–N(2)	139.8 (2)
O(2)–Mn(1)–N(2)	84.2 (1)	N(1)–Mn(1)–N(2)	91.0 (2)
O(1)–Mn(2)–O(2)	71.6 (1)	O(1)–Mn(2)–N(3)	140.0 (2)
O(2)–Mn(2)–N(3)	85.5 (1)	N(3)–Mn(2)–N(4)	78.3 (2)
O(2)–Mn(2)–N(4)	86.3 (1)	O(1)–Mn(2)–N(4)	130.3 (2)
O(1)–Mn(2)–N(5)	85.9 (1)	O(2)–Mn(2)–N(5)	122.2 (1)
N(3)–Mn(2)–N(5)	79.1 (1)	N(4)–Mn(2)–N(5)	141.6 (2)
O(1)–Mn(2)–N(6)	94.5 (1)	O(2)–Mn(2)–N(6)	155.6 (1)
N(3)–Mn(2)–N(6)	116.5 (2)	N(4)–Mn(2)–N(6)	88.1 (2)
N(5)–Mn(2)–N(6)	75.0 (2)	Mn(1)–O(1)–C(16)	129.9 (3)
Mn(1)–O(2)–C(5)	131.8 (3)	Mn(2)–O(1)–C(16)	118.7 (3)
Mn(2)–O(2)–C(5)	118.1 (3)		

ring chelates with twisted conformations.

8. Discussion

Although the synthetic objectives of generating homo- and heterobimetallic complexes with metals in closed and open sites have been achieved, the systems require modification in order to obtain the desired reactivity and stereochemistry. In view of the present results it seems probable that nonmacrocyclic ligand systems will form symmetrical bimetallic complexes. Thus, for example, replacing the aldehyde groups with appropriate donor ligands should give symmetrical bimetallic complexes. The present set of donor atoms do not facilitate the oxidation of the bound metals. For dioxygen uptake studies it seems that more basic and/or negatively charged donor atoms are required. Our inability to oxidize both Mn(II) ions of $[\text{Mn}(\text{cyclim})\text{MnCl}]^+$ suggests that the oxidation of one metal leads to the deactivation of the second metal to oxidation. This phenomenon has been observed before.²¹

(21) Schenck, T. G.; Milne, C. R. C.; Sawyer, J. F.; Bosnich, B. *Inorg. Chem.* 1985, 24, 2338.

Since in the present ligand type it is the closed-site metal that is the more difficult to oxidize, the oxidative inertness of this site may be circumvented by incorporating either a more oxidizable metal or by adjusting the surrounding ligands or both. We note that the Robson ligand, which cyclim resembles, strongly stabilizes lower oxidation state metals.¹⁴

The observation that both metals may participate as epoxidation catalysts may be connected with the unsymmetrical structure of the bimetallic systems. The asymmetry may indicate a strained coordination environment. This, together with the inherent lability of spin-free Mn(II) could account for the direct participation of the closed site in epoxidation. It would be interesting to see if the closed site participated directly in epoxidation if it were less strained.

Finally, the synthesis of these types of ligands is elaborate and requires greater dispatch and efficiency. More efficient routes to ligand synthesis are in hand, and the other questions raised in this study will be addressed in future papers.

9. Experimental Section

¹H NMR spectra were obtained either on a General Electric QE 300 or a Chicago-built 500 Fourier transform spectrometer. UV spectra were recorded on a Varian (Cary) 2400 spectrophotometer using spectral grade solvents. IR spectra were run as Nujol mulls on a Nicolet 20 SXB FT-IR spectrometer. Magnetic susceptibilities of powdered samples were measured using a Johnson Matthey Evans magnetic susceptibility balance. Susceptibilities of samples in solution were obtained in CD₂Cl₂ or CD₃CN with coaxial NMR tube inserts according to the Evans method,¹⁶ using the above-mentioned constant-field GE QE 300 NMR instrument. Conductance measurements were made with a YSI Model 35 conductance meter. Elemental analyses were performed by Huffman Laboratories, Golden, CO, or Desert Analytics, Tucson, AZ. Solvents used in preparative reactions were dried over CaH₂ (CH₂Cl₂, Et₃N, DMSO), K (THF), or LiAlH₄ (ether, 1,4-dioxane). Air-sensitive Co and Mn complexes were prepared under argon, using deaerated solvents and standard Schlenk techniques.

Ligand Synthesis. 2,6-Bis(hydroxymethyl)-4-methylphenol (9). Triol **9** was made by a modification of the preparation described by Ullmann.¹⁰ *p*-Cresol (54 g, 0.5 mol) was added to a stirred aqueous NaOH solution (6.25 M, 100 mL). After a golden color developed (5–10 min), a 37% formaldehyde solution (99.3 mL, 1.33 mol) was added. The solution was stirred for 20 min. Over time a pale yellow solid formed in the bright yellow solution. After 24 h the entire solid reaction mixture was diluted with 200 mL of H₂O, and was stirred and sonicated. It was then acidified to pH 6 with HCl (12 M, 48 mL). The white solid suspension was stirred vigorously for 1 h, after which time it was filtered and washed with H₂O (3 × 350 mL). The white tacky solid was dried first by suction on the sinter and then in a vacuum desiccator. The product was purified by recrystallization from a 1:1 hot acetone–hexane mixture (5 mL of acetone per gram of crude solid). The triol **9** was obtained as very pale yellow crystals: 40.6 g (48%). ¹H NMR (CDCl₃): δ 2.24 (s, 3 H), 2.30 (t, *J* = 6.0 Hz, 2 H), 4.76 (d, *J* = 6.0 Hz, 4 H), 6.86 (s, 2 H), 7.75 (s, 1 H).

2,2-Dimethyl-6-methyl-8-(hydroxymethyl)benzo-1,3-dioxin (10). Triol **9** (25.0 g, 0.15 mol) was suspended in dry THF (125 mL) under nitrogen and several drops of 99% methanesulfonic acid were added.²² 2-Methoxypropene (12.2 g, 0.17 mol) in THF (10 mL) was added dropwise to the suspension. The resultant pale yellow solution was stirred for 24 h and then was poured into dilute NaOH (1.3 M, 150 mL) and extracted with benzene (3 × 125 mL). The combined organic fractions were washed with H₂O until the washes were neutral and then with brine (1 × 300 mL) and were then dried over MgSO₄. After filtration and concentration in vacuo, a very pale yellow oil, **10**, was obtained, which crystallized over time: 31.8 g (95%). ¹H NMR (CDCl₃): δ 1.53 (s, 6 H), 2.17 (t, *J* = 7.5 Hz, 1 H), 2.26 (s, 3 H), 4.59 (d, *J* = 7.5 Hz, 2 H), 4.82 (s, 2 H), 6.72 (s, 1 H), 6.97 (s, 1 H).

2,2-Dimethyl-6-methyl-8-formylbenzo-1,3-dioxin (11). Method 1.¹¹ A stirred solution of oxalyl chloride (7.41 g, 0.057 mol) in dry distilled CH₂Cl₂ (100 mL) under argon was cooled to –60 °C in a dry ice/2-propanol bath. Dimethyl sulfoxide (8.98 g, 0.115 mol) in CH₂Cl₂ (15 mL) was added slowly dropwise to the cooled solution. The acetonide **10** (10.0 g, 0.048 mol) in CH₂Cl₂ (25 mL) and DMSO (1–2 mL) was added slowly dropwise. The white cloudy mixture was stirred at –60 °C for 20 min, and then dry Et₃N (24.18 g, 0.239 mol) was added dropwise. The thick yellow mixture was allowed to warm to room temperature and was then quenched with H₂O (100 mL). The phases were separated and

the aqueous layer was extracted with CH₂Cl₂ (2 × 75 mL). The combined organic layers were concentrated under reduced pressure, and the resultant yellow residue was dissolved in ether (150 mL) and washed with H₂O (3 × 150 mL) and then with brine (1 × 150 mL) and was dried over MgSO₄. Filtration and concentration under reduced pressure yielded crude **11** as a yellow oil: 9.68 g (98%).

Method 2.¹² To the protected alcohol **10** (20 g, 0.096 mol) in CH₂Cl₂ (220 mL) was added Chlorox bleach (5.25% NaOCl, 600 mL) followed by *n*Bu₄NBr (6.2 g, 0.020 mol). After 2 h of very vigorous stirring to obtain a finely dispersed mixture, the two layers were separated, the aqueous layer was extracted with additional CH₂Cl₂ (2 × 100 mL), and the combined organic layers were concentrated on the rotary evaporator. The resultant amber residue was shaken with an ether–pentane–H₂O mixture (600 mL–200 mL–200 mL). After separation, the organic phase was washed with aqueous NaOH (0.5 M, 5 × 200 mL), H₂O (3 × 200 mL), and brine (2 × 150 mL) and then was dried over Na₂SO₄. Filtration and concentration yielded crude **11**, a light yellow oil, sufficiently pure for the next reaction: ~14.85 g (~75%). ¹H NMR (CDCl₃): δ 1.60 (s, 6 H), 2.27 (s, 3 H), 4.83 (s, 2 H), 6.97 (s, 1 H), 7.48 (s, 1 H), 10.33 (s, 1 H).

2-Hydroxy-3-(hydroxymethyl)-5-methylbenzaldehyde (12). Formic acid (70%, 220 mL) was added to the aldehyde **11** (18.68 g, 0.091 mol). After being stirred for 2 h, the reaction mixture was poured into ether (~200 mL), and H₂O was added until two layers separated. The aqueous phase was extracted with ether (2 × 100 mL). Combined organic fractions were shaken with saturated aqueous NaHCO₃ until washes were neutral and were dried over MgSO₄, filtered, and then concentrated in vacuo. The residue was dissolved in methanol (130 mL) and aqueous NaOH (1.44 M, 130 mL) was added to the stirred solution. After 30 min the bright yellow-orange reaction solution was neutralized with concentrated aqueous HCl (12 M, ~16 mL). The mixture was extracted with ether (2 × 150 mL), and the combined ether extracts were shaken with brine (1 × 200 mL) and were dried over MgSO₄, filtered, were concentrated in vacuo to give crude **12** as a yellow solid: 13.44 g (89%). ¹H NMR (CDCl₃): δ 2.28 (br t, *J* = 5.5 Hz, 1 H), 2.33 (s, 3 H), 4.72 (d, *J* = 5.1 Hz, 2 H), 7.26 (s, 1 H), 7.37 (s, 1 H), 9.82 (s, 1 H), 11.13 (s, 1 H).

2-(Allyloxy)-3-(hydroxymethyl)-5-methylbenzaldehyde (13). Aqueous NaOH (0.65 M, 150 mL) was added to a stirred solution of the phenol **12** (13.44 g, 0.081 mol) in CH₂Cl₂ (150 mL) under nitrogen.²³ Allyl bromide (11.74 g, 0.097 mol) and *n*Bu₄NBr (13.04 g, 0.040 mol) were added. After 24 h of vigorous stirring, the layers were separated, the aqueous layer was extracted with CH₂Cl₂ (2 × 75 mL), and the combined organic layers were concentrated in vacuo. The residue was dissolved in ether (150 mL), washed with H₂O (4 × 100 mL), shaken with brine (1 × 150 mL), and dried over MgSO₄. Filtration and concentration under reduced pressure yielded **13** as a yellow oil: 16.02 g (96%). ¹H NMR (CDCl₃): δ 1.95 (t, *J* = 5.6 Hz, 1 H), 2.34 (s, 3 H), 4.47 (d, *J* = 5.7 Hz, 2 H), 4.71 (d, *J* = 5.6 Hz, 2 H), 5.29 (d, *J* = 10.5 Hz, 1 H), 5.39 (d, *J* = 16.6 Hz, 1 H), 6.10 (m, 1 H), 7.46 (s, 1 H), 7.53 (s, 1 H), 10.27 (s, 1 H).

2-(Allyloxy)-3-(chloromethyl)-5-methylbenzaldehyde (14). A stirred solution of *N*-chlorosuccinimide (7.13 g, 0.053 mol) in dry distilled CH₂Cl₂ (225 mL) was cooled to 0 °C. Dimethyl sulfide (3.65 g, 0.059 mol) was added dropwise. The white reaction mixture was further cooled to –25 °C and the alcohol **13** (10.0 g, 0.049 mol) in dry distilled CH₂Cl₂ (10 mL) was added slowly dropwise.²⁴ After being stirred at 0 °C for 2 h, the reaction was poured into ice cold brine (~200 mL), the aqueous layer was extracted with ether (2 × 100 mL), and the combined organic layers were dried over MgSO₄. Filtration and concentration under reduced pressure gave crude **14** as a pale yellow solid (11.69 g). The crude solid was purified by "filtration" through a short column (basic alumina, activity I, 50 g, 5 in.). The compound was dissolved and loaded in ether–hexane (60:40) and eluted with a 70:30 mixture. The yellow solid (8.92 g) obtained from concentration of appropriate column fractions was triturated with cold hexane to remove yellow impurities, collected, and washed with cold hexane and then was dried in a vacuum desiccator. Pure product was obtained as a fluffy white crystalline solid: 6.55 g (60%, based on starting alcohol **13**). An analytical sample was obtained by recrystallization from ether–hexane. Anal. Calcd for C₁₂H₁₃O₂Cl: C, 64.15; H, 5.83; Cl, 15.78. Found: C, 64.16; H, 5.96; Cl, 15.84. ¹H NMR (CDCl₃): δ 2.38 (s, 3 H), 4.58 (d, *J* = 5.7 Hz, 2 H), 4.66 (s, 2 H), 5.35 (dd, *J* = 10.3, 1.4 Hz, 1 H), 5.46 (dd, *J* = 17.1, 1.4 Hz, 1 H), 6.11 (m, 1 H), 7.52 (d, *J* = 2.2 Hz, 1 H), 7.64 (d, *J* = 2.2 Hz, 1 H), 10.32 (s, 1 H).

2-(Allyloxy)-3-(chloromethyl)-5-methylbenzaldehyde, Dimethyl Acetal (15). The chloride **14** (6.19 g, 0.028 mol), trimethyl orthoformate (9.35

(22) Greene, T. H. *Protective Groups in Organic Synthesis*; John Wiley & Sons: New York, 1981; p 76.

(23) McKillop, A.; Fiaud, J.-C.; Hug, R. P. *Tetrahedron* 1974, 30.

(24) Corey, E. J.; Kim, C. U.; Takeda, M. *Tetrahedron Lett.* 1972, 4339.

g, 0.088 mol), and *p*-toluenesulfonic acid (0.26 g, 0.0014 mol) were dissolved in methanol (140 mL) and were stirred for 20 h under nitrogen. The reaction mixture was poured into a cooled, stirred phosphate buffer solution (pH 7.0, 300 mL) and then was extracted with ether (2 × 200 mL). The combined ether extracts were washed with H₂O (2 × 200 mL) and brine (1 × 200 mL) and were dried over MgSO₄. Filtration and concentration under reduced pressure gave crude **15**, a golden yellow oil: 7.36 g (~100%). ¹H NMR (CDCl₃): δ 2.32 (s, 3 H), 3.36 (s, 6 H), 4.47 (d, *J* = 5.9 Hz, 2 H), 4.61 (s, 2 H), 5.28 (dd, *J* = 10.5, 1.4 Hz, 1 H), 5.45 (dd, *J* = 17.1, 1.4 Hz, 1 H), 5.55 (s, 1 H), 6.11 (m, 1 H), 7.19 (s, 1 H), 7.30 (s, 1 H).

1,6-Bis(2-pyridyl)-2,5-bis(2-allyloxy)-3-formyl-5-methylbenzyl)-2,5-diazahexane (17). 1,6-Bis(2-pyridyl)-2,5-diazahexane (**16**) (3.06 g, 0.013 mol)²⁵ and the acetal **15** (7.36 g, 0.027 mol) were dissolved in dry distilled 1,4-dioxane (200 mL) under nitrogen, and anhydrous Na₂CO₃ (11.66 g, 0.110 mol) was added. The reaction mixture was stirred at 100 °C for 2 days, was allowed to cool to room temperature, and then was filtered through Celite. Dioxane was removed by concentration in vacuo to give a very thick orange-brown oil, which was treated with aqueous HCl (1.16 M, 222 mL) and heated on a steam bath for 10 min. After cooling, the brown suspension was extracted with ether (4 × 100 mL). The aqueous layer was taken to pH ~7.0 with aqueous NaOH and then to pH ~8.4 by addition of saturated aqueous NaHCO₃. The oily mixture was extracted with CH₂Cl₂ (~8 × 50 mL), and the combined organic extracts were dried over Na₂SO₄. Filtration and concentration under reduced pressure gave essentially pure dialdehyde **17** as a very viscous orange-brown oil: 8.32 g (~100%). ¹H NMR (CDCl₃): δ 2.24 (s, 6 H), 2.69 (s, 4 H), 3.63 (s, 4 H), 3.72 (s, 4 H), 4.33 (d, *J* = 6.5 Hz, 4 H), 5.23 (d, *J* = 10.4 Hz, 2 H), 5.32 (d, *J* = 17.0 Hz, 2 H), 5.96 (m, 2 H), 7.08 (m, 2 H), 7.33 (d, *J* = 7.8 Hz, 2 H), 7.47 (s, 2 H), 7.49 (s, 2 H), 7.53 (m, 2 H), 8.44 (d, *J* = 4.5 Hz, 2 H), 10.22 (s, 2 H).

1,6-Bis(2-pyridyl)-2,5-bis(2-hydroxy-3-formyl-5-methylbenzyl)-2,5-diazahexane (6).¹³ A dry THF solution (150 mL) of the allyl compound **17** (7.98 g, 0.0129 mol) and [Pd(PPh₃)₄] (0.5 g, 0.43 mmol) was stirred under argon. To this mixture was added via cannula a dry THF solution (~100 mL) of sodium dimethyl malonate, prepared from dimethyl malonate (7.11 g, 0.054 mol) and NaH (0.81 g, 80% suspension in mineral oil, 0.027 mol). The resultant chestnut-brown solution was stirred for 1.5 h, and quenched with aqueous HCl (1 M, 35 mL), and the THF was removed in vacuo. After acidification with HCl (1 M, 165 mL), the aqueous layer was shaken with ether (200 mL) and gravity filtered and then was further extracted with ether (4 × 75 mL). The aqueous layer was taken to pH ~7 with aqueous NaOH and then to pH ~8.4 with saturated aqueous NaHCO₃. It was extracted with CH₂Cl₂ (8 × 50 mL). The combined CH₂Cl₂ fractions were dried over Na₂SO₄ and filtered and were concentrated under reduced pressure to give crude **6** as a very viscous orange-brown oil (6.64 g).

Purification of 6. Step A. To an absolute ethanol solution (30 mL) of the crude dialdehyde **6** (6.63 g, 0.0123 mol) was added a methanol solution (30 mL) of Zn(OAc)₂·2H₂O (2.79 g, 0.0127 mol) and Et₃N (2.57 g, 0.025 mol). The resultant yellow precipitate was stirred for ~5 h. It was collected and washed with methanol (2 × 10 mL), absolute ethanol (2 × 10 mL), ether (3 × 10 mL), and pentane (2 × 10 mL), and was dried in a vacuum desiccator, yielding the mono Zn complex [Zn-(pyral)] as shiny yellow plates: 4.48 g. A second crop of mono Zn complex was obtained upon removal of the solvent. The residue was slurried in absolute ethanol (~10 mL) and collected and washed as above to yield a slightly darker yellow crystalline solid: 0.68 g (70% combined yield).

Step B. Pure free ligand **6** was liberated from the mono Zn complex by the following method. H₂S(g) was bubbled slowly for ~2 min through a stirred suspension of the mono Zn complex (0.5 g, 0.83 mmol) in dry distilled CH₂Cl₂ (~30 mL). After 1 h, the suspension was filtered through Celite and the CH₂Cl₂ was removed under reduced pressure. The yellow-orange residue was dissolved in methanol (~30 mL), sonicated, and filtered through Celite and was then concentrated under reduced pressure to give the pure dialdehyde ligand **6** as a yellow oil: 0.39 g (87%). ¹H NMR (CDCl₃): δ 2.22 (s, 6 H), 2.74 (s, 4 H), 3.64 (s, 4 H), 3.72 (s, 4 H), 7.10 (s, 2 H), 7.13 (m, 2 H), 7.21 (d, *J* = 7.8 Hz, 2 H), 7.33 (s, 2 H), 7.56 (m, 2 H), 8.49 (d, *J* = 4.6 Hz, 2 H), 10.14 (s, 2 H), 11.5 (br s, 2 H).

Monometal Complexes. [Zn(pyral)]. See preparation given above. An analytical sample of the mono Zn complex was obtained by the following method. The yellow solid was dissolved in a minimal amount of a hot 1:1 CH₂Cl₂-absolute ethanol mixture and the CH₂Cl₂ was boiled off. Upon cooling, the yellow crystals were collected and washed as above (97% recovery). Anal. Calcd for C₃₂H₃₂O₄N₄Zn: C, 63.84; H, 5.36;

N, 9.31; Zn, 10.86. Found: C, 63.28; H, 5.41; N, 9.14; Zn, 9.74. ¹H NMR (CD₂Cl₂): δ 2.12 (s, 6 H), 2.83 (s, 4 H), 3.37 (d, *J* = 11.6 Hz, 2 H), 3.76 (d, *J* = 16.9 Hz, 2 H), 4.05 (d, *J* = 16.5 Hz, 2 H), 4.06 (d, *J* = 12.1 Hz, 2 H), 6.84 (d, *J* = 7.8 Hz, 2 H), 6.92 (d, *J* = 2.9 Hz, 2 H), 7.16 (d, *J* = 1.4 Hz, 2 H), 7.10 (m, 2 H), 7.58 (m, 2 H), 8.95 (dd, *J* = 4.8, 0.6 Hz, 2 H), 10.33 (s, 2 H).

[Co(pyral)]. All solvents used in the following preparation were deaerated and all procedures were conducted under argon. Co(OAc)₂·4H₂O (0.20 g, 0.8 mmol) in methanol (5 mL) was added dropwise to a yellow ethanol solution (8 mL) of free dialdehyde **6** (0.41 g, 0.76 mmol). An orange solid formed almost immediately. The suspension was stirred for 2–3 min followed by addition of Et₃N (0.15 g, 0.76 mmol). Stirring was continued for 10 min. The tacky orange solid was collected by filtration, washed with ethanol (3 × 3 mL), ether (3 × 3 mL) and pentane (3 × 3 mL), and then dried under a stream of nitrogen. The crude product was recrystallized from CH₂Cl₂-ethanol by slow evaporation to yield orange-red crystals: 0.15 g. A second crop of crystals was obtained by concentrating the filtrate and repeating the aforementioned procedure: 0.07 g. Pure product was collected and washed as above and then dried under high vacuum for 1–2 h (49% combined yield). The mono Co complex is air stable as a solid. Anal. Calcd for C₃₂H₃₂O₄N₄Co: C, 64.54; H, 5.42; N, 9.41; Co, 9.89. Found: C, 64.46; H, 5.44; N, 9.35; Co, 9.67.

[Mn(pyral)]. The mono Mn complex was prepared and recrystallized by the same method used for the mono Co complex except that after the reagents were combined, the mixture was stirred for 3 h. The orange-yellow crystals were collected and washed successively with ethanol, ether, and pentane. After recrystallization, air-stable orange needles were obtained (75% combined yield). Anal. Calcd for C₃₂H₃₂O₄N₄Mn: C, 64.97; H, 5.45; N, 9.47; Mn, 9.29. Found: C, 64.61; H, 5.80; N, 9.44; Mn, 9.05.

[Co(pyral)]PF₆. [Co(pyral)] (7.68 mg, 0.013 mmol) and Cp₂Fe(PF₆) (4.29 mg, 0.013 mmol) were weighed into an NMR tube equipped with a rubber septum cap. The tube was flushed with argon for 3 min. CD₃CN (0.4 mL) was added via a syringe. Dissolution of the solids and immediate reaction resulted in a dark brown solution. ¹H NMR (CD₃CN): δ 2.14 (s, 6 H), 3.28 (s, 4 H), 3.52, 3.62 (syst AB, *J*_{AB} = 14 Hz, 2 H), 4.43, 4.59 (syst AB, *J*_{AB} = 19 Hz, 2 H), 7.02 (s, 2 H), 7.22 (s, 2 H), 7.32 (d, *J* = 7.8 Hz, 2 H), 7.43 (t, *J* = 6.6 Hz, 2 H), 7.89 (t, *J* = 7.6 Hz, 2 H), 8.60 (d, *J* = 5.7 Hz, 2 H), 10.40 (s, 2 H).

Homobimetallic Complexes. Homobimetallic complexes were prepared by the following general procedure. Any variations from this method will be indicated for the corresponding metal complex. For preparations of cobalt and manganese complexes all solvents were deaerated and all procedures were conducted under argon. The free dialdehyde ligand **6** (0.74 mmol) was dissolved in absolute ethanol (10 mL), and the bright yellow solution was cannulated into a 3-neck flask (equipped with a reflux condenser and an addition funnel) containing the metal acetate (1.56 mmol). The stirred solution was heated to 60 °C followed by slow dropwise addition of an ethanol solution (5 mL) containing 1,3-diaminopropane (0.780 mmol). Stirring was continued at 60 °C for 2 h, Et₃N (1.52 mmol) was added, and then the reaction was heated to reflux. The counterions, NH₄PF₆ (3.7 mmol) for (PF₆)₂ complexes, or LiCl (3.0 mmol) and NH₄PF₆ (3.7 mmol) combined for chloro-PF₆ complexes, were dissolved in a minimal amount of methanol. The salt solution was filtered through a cotton plug and added dropwise to the refluxing reaction solution. Reflux was maintained for 45 min, and then the reaction was allowed to cool slowly to room temperature. For (PF₆)₂ complexes a solid precipitated out of solution immediately upon addition of the counterions. For chloro-PF₆ complexes either concentration or cooling or both were required before the product precipitated. The crude solids were collected under argon, washed with ethanol (3 × 3 mL), Et₂O (3 × 3 mL), and pentane (3 × 3 mL) then dried under a steady stream of nitrogen. The dry bimetallic complexes are stable in air. The purification of these complexes is described later.

Heterobimetallic Complexes. All heterobimetallic complexes were prepared according to the following general method. Preparations of complexes containing cobalt or manganese were conducted under argon and all solvents were deaerated. To a stirred methanol suspension (10 mL) of the appropriate mono metal complex (0.83 mmol) was added slowly dropwise a methanol solution containing 1,3-diaminopropane (0.87 mmol) and glacial acetic acid (1.74 mmol). The reaction was stirred at room temperature for 2 h and then was neutralized by addition of Et₃N (1.74 mmol). The metal acetate corresponding to the desired open-site metal was dissolved in methanol (5 mL) and added slowly dropwise to the "precyclized" mono metal complex at 25 °C. The solution was stirred for 15 min. A filtered solution of NH₄PF₆ (4.2 mmol) and LiCl (3.3 mmol) dissolved in a minimal amount of methanol was added to the reaction solution. The mixture was then warmed to 50–60 °C for 30 min under a slow steady stream of nitrogen to decrease the solvent volume.

After gradual cooling, the solid product was collected by filtration under argon and washed with ethanol (3×3 mL), ether (3×3 mL), and pentane (3×3 mL) and then was dried under a slow stream of nitrogen. If yields of precipitated product were low, the reaction filtrate was concentrated to dryness. The residues so obtained were dissolved in warm CH_3CN and filtered to remove any insoluble salts or solids, and then the solution was added to any initially collected solid for recrystallization.

Purification. All bimetallic complexes were purified by recrystallization from CH_3CN -ethanol (with the exception of $[\text{Zn}(\text{cyclim})\text{Zn}](\text{PF}_6)_2$ which could only be crystallized from CH_3CN -ether). The $(\text{PF}_6)_2$ salts were crystallized by dissolution of the crude solids in a minimal amount of CH_3CN (~ 5 mL for ~ 0.35 g of complex) and precipitation was induced with absolute ethanol (10–15 mL). When the mixture was allowed to stand, large crystals were obtained. To obtain good crystals of the chloro- PF_6 complexes in reasonable yield the following procedure was followed. The crude product was dissolved in a minimal amount of hot CH_3CN (~ 15 mL per ~ 0.35 g of complex), and the hot solution was filtered. To the CH_3CN solution, maintained at $\sim 80^\circ\text{C}$ in a warm water bath, was added an approximately equal volume of ethanol. (Less ethanol was added if crystallization commenced prior to addition of an equal volume). A very slow steady stream of nitrogen was passed over the hot solution to further reduce the CH_3CN content, and additional aliquots of ethanol ($\sim 3 \times 3$ mL) were added over time. Crystals began to form slowly in the hot solution. After approximately one-third of the solid submitted had recrystallized out of solution, the heating was turned off and the flask was allowed to cool very slowly in the water bath. (Note: Yields were very low if the solution was allowed to stand and cool upon the first appearance of crystals.) Once the solution had reached room temperature, the nitrogen stream was turned off and the flask was sealed under argon and allowed to stand, typically overnight. Crystals were collected, washed with ethanol (3×3 mL), ether (3×3 mL), and pentane (3×3 mL), and then dried under high vacuum for 5–6 h. Reported yields are calculated after recrystallization and are based on free ligand for homobimetallic complexes. For heterobimetallic compounds yields are based upon the pure mono metal complex submitted.

$[\text{Zn}(\text{cyclim})\text{Zn}](\text{PF}_6)_2 \cdot \text{CH}_3\text{CN}$. The yellow solid was recrystallized from CH_3CN -ether to give opaque yellow crystals. Yield: 66%. $\Delta_M = 290 \text{ cm}^2 \Omega^{-1} \text{ mol}^{-1}$ in CH_3CN . ^1H NMR (CD_3CN): δ 2.12 (s, 6 H), 2.21 (br, 2 H), 3.22 (m, 2 H), 3.42 (br, 2 H), 3.55 (d, $J = 11.5$ Hz, 2 H), 3.91 (br, 2 H), 4.04 (m, 6 H), 4.56 (br, 2 H), 6.76 (s, 2 H), 6.90 (d, $J = 7.54$ Hz, 2 H), 7.06 (s, 2 H), 7.11 (t, br, 2 H), 7.56 (t, $J = 7.53$ Hz, 2 H), 8.06 (br, 2 H), 8.22 (d, $J = 3.51$ Hz, 2 H). Anal. Calcd for $\text{C}_{37}\text{H}_{40}\text{O}_2\text{N}_6\text{P}_2\text{F}_{12}\text{Zn}_2$: C, 42.88; H, 3.99; N, 9.46. Found: C, 43.10; H, 4.26; N, 9.53.

$[\text{Co}(\text{cyclim})\text{Co}](\text{PF}_6)_2 \cdot 2\text{CH}_3\text{CN}$. Large dark red-brown crystals were obtained upon recrystallization. Yield: 55%. $\Delta_M = 276 \text{ cm}^2 \Omega^{-1} \text{ mol}^{-1}$ in CH_3CN . Anal. Calcd for $\text{C}_{39}\text{H}_{44}\text{O}_2\text{N}_6\text{P}_2\text{F}_{12}\text{Co}_2$: C, 43.96; H, 4.16; N, 10.52; Co, 11.06. Found: C, 44.23; H, 4.52; N, 10.22; Co, 11.60.

$[\text{Co}(\text{cyclim})\text{CoCl}](\text{PF}_6)$. The complex crystallized as brown rectangular blocks. Yield: 45%. $\Delta_M = 134 \text{ cm}^2 \Omega^{-1} \text{ mol}^{-1}$ in CH_3CN . Anal. Calcd for $\text{C}_{35}\text{H}_{38}\text{O}_2\text{N}_6\text{ClPF}_6\text{Co}_2$: C, 48.15; H, 4.39; N, 9.63; Cl, 4.06; Co, 13.50. Found: C, 48.47; H, 4.81; N, 9.72; Cl, 3.97; Co, 13.96.

$[\text{Mn}(\text{cyclim})\text{MnCl}](\text{PF}_6)$. Fine yellow-orange needles were obtained after recrystallization. Yield: 67%. $\Delta_M = 132 \text{ cm}^2 \Omega^{-1} \text{ mol}^{-1}$ in CH_3CN . Yellow-orange rectangular blocks suitable for X-ray crystal structure determination were grown under argon by vapor diffusion of ether into a CH_3CN solution of the complex. Anal. Calcd for $\text{C}_{35}\text{H}_{38}\text{O}_2\text{N}_6\text{ClPF}_6\text{Mn}_2$: C, 48.60; H, 4.43; N, 9.72; Cl, 4.10; Mn, 12.70. Found: C, 48.72; H, 4.61; N, 9.72; Cl, 4.22; Mn, 11.92.

$[\text{Zn}(\text{cyclim})\text{CoCl}](\text{PF}_6) \cdot \text{H}_2\text{O}$. The complex was recrystallized to give fine golden-brown needles. Yield: 59%. $\Delta_M = 126 \text{ cm}^2 \Omega^{-1} \text{ mol}^{-1}$ in CH_3CN . Anal. Calcd for $\text{C}_{35}\text{H}_{40}\text{O}_3\text{N}_6\text{ClPF}_6\text{ZnCo}$: C, 46.89; H, 4.50; N, 9.37; Zn, 7.29; Co, 6.57. Found: C, 46.78; H, 4.79; N, 9.43; Zn, 7.64; Co, 6.35.

$[\text{Zn}(\text{cyclim})\text{MnCl}](\text{PF}_6)$. The complex was recrystallized to give yellow-orange needles. Yield: 57%. $\Delta_M = 133 \text{ cm}^2 \Omega^{-1} \text{ mol}^{-1}$ in CH_3CN . Anal. Calcd for $\text{C}_{35}\text{H}_{38}\text{O}_2\text{N}_6\text{ClPF}_6\text{ZnMn}$: C, 48.02; H, 4.37; N, 9.60; Cl, 4.05; Zn, 7.47; Mn, 6.28. Found: C, 48.25; H, 4.60; N, 9.55; Cl, 4.24; Zn, 6.79; Mn, 7.04.

$[\text{Mn}(\text{cyclim})\text{ZnCl}](\text{PF}_6)$. The complex gave large orange needles. Yield: 69%. $\Delta_M = 124 \text{ cm}^2 \Omega^{-1} \text{ mol}^{-1}$ in CH_3CN . Anal. Calcd for $\text{C}_{35}\text{H}_{38}\text{O}_2\text{N}_6\text{ClPF}_6\text{MnZn}$: C, 48.02; H, 4.37; N, 9.60; Cl, 4.05; Mn, 6.28; Zn, 7.47. Found: C, 48.38; H, 4.46; N, 9.53; Cl, 4.10; Mn, 5.02; Zn, 7.32.

$[\text{Mn}(\text{cyclim})(\mu\text{-Cl})\text{MnCl}](\text{PF}_6) \cdot 0.5\text{CH}_3\text{CN}$. Method 1. The $[\text{Mn}(\text{cyclim})\text{MnCl}](\text{PF}_6)$ complex (0.120 g, 0.14 mmol) was dissolved in CH_3CN (7 mL). A methanol solution (0.5 mL) of LiCl (7.2 mg, 0.17 mmol) was added. A very slow steady stream of $\text{O}_2(\text{g})$ was bubbled through the stirred mixture for 24 h. During this time the bright yellow solution darkened to very dark orange-brown. The dark solution was filtered and

then was subjected to vapor diffusion with ether. After 1–3 days black-brown diamond-shaped crystals were collected and washed with 10% CH_3CN in ether (3×3 mL), ether (3×3 mL), and pentane (3×3 mL) and then were dried under high vacuum for 5 h: 0.0828 g (62%).

Method 2. $[\text{Mn}(\text{cyclim})\text{MnCl}](\text{PF}_6)$ (0.2248 g, 0.26 mmol) was dissolved in deaerated CH_3CN (10 mL) and combined with a methanol solution of LiCl (12.1 mg, 0.29 mmol). To this mixture, stirred under argon, was added slowly dropwise a CH_3CN solution (3 mL) of $\text{Cp}_2\text{Fe}(\text{PF}_6)$ (0.095 g, 0.29 mmol). The initial yellow complex solution turned yellow-brown. The reaction was stirred for 1.5 h and then was concentrated to dryness. The brown residue was triturated with ether ($\sim 5 \times 5$ mL) until washes were no longer yellow and all of the Cp_2Fe had been removed. The crude product was purified by successive recrystallizations, first from acetone-ethanol, followed by a vapor diffusion crystallization from CH_3CN -ether. Dark black-brown crystals were collected, washed, and dried as described for method 1: 0.190 g (78%). $\Delta_M = 126 \text{ cm}^2 \Omega^{-1} \text{ mol}^{-1}$ in CH_3CN . Anal. Calcd for $\text{C}_{36}\text{H}_{39.5}\text{O}_2\text{N}_6\text{PF}_6\text{Mn}_2$: C, 46.95; H, 4.32; N, 9.88; Cl, 7.70; Mn, 11.93. Found: C, 46.77; H, 4.36; N, 9.87; Cl, 7.62; Mn, 9.56.

Styrene Epoxidation. Epoxidation reactions were run as follows. Approximately 1.50×10^{-6} mol of metal complex was weighed into an NMR tube equipped with a rubber septum cap. The tube was flushed with argon and sufficient CD_3CN was added via syringe to make a 3 mM solution of catalyst. Styrene was added via syringe, and a spectrum was recorded. PhIO was added quickly all at once, the NMR tube was again flushed with argon, and the heterogeneous mixture was sonicated for 2–3 min. The course of the reaction was monitored by NMR.

X-ray Structure Determination of $[\text{Co}(\text{cyclim})\text{Co}](\text{PF}_6)_2$ (1), $[\text{Mn}(\text{cyclim})(\mu\text{-Cl})\text{MnCl}](\text{PF}_6)$ (2), $[\text{Co}(\text{cyclim})\text{CoCl}](\text{PF}_6)$ (3), and $[\text{Mn}(\text{cyclim})\text{MnCl}](\text{PF}_6)$ (4). Crystal, data collection, and refinement parameters are collected in Table III. Single crystals of 1–4 were each mounted on fine glass fibers with epoxy cement. The unit cell parameters for each crystal were obtained from the least-squares fit of 25 reflections ($20^\circ \leq 2\theta \leq 25^\circ$). Preliminary photographic characterizations showed *mmm* Laue symmetry for 1 and *2/m* Laue symmetry for 2–4. The systematic absences in the diffraction data of 1 uniquely established the space group as *Pbca* (No. 61). The systematic absences in the diffraction data of 3 and 4 uniquely established the space groups as $P2_1/n$ (No. 14) for both 3 and 4. The systematic absences in the diffraction data of 2 established the space group as $P2_1$ (No. 4) or $P2_1/m$ (No. 11). The *E* statistics suggested the noncentrosymmetric alternative $P2_1$, and the chemically sensible results of refinement indicated that this choice is correct. The refinement of a multiplicative term (0.941) for $\Delta f''$ for 2 indicated that the enantiomer reported is correct. An absorption correction was not applied to the data sets of 1, 2, or 4 but the semiempirical absorption correction program XABS was applied to the data set of 3.

Structure Solution and Refinement. 1 was solved by direct methods which located the Co atoms. 2 was solved by direct methods which located the Mn atoms. 3 was solved by means of a Patterson map which located the Co atoms. The remaining non-hydrogen atoms of 1–3 were located through subsequent least-squares and difference Fourier syntheses. Since 4 is isostructural with 3, 4 was solved by using the non-hydrogen atom coordinates of 3, replacing the Co atoms with Mn atoms in the atom list and allowing the structure to refine. In all of these structures all hydrogens were included as idealized isotropic contributions ($d(\text{CH}) = 0.960 \text{ \AA}$, $U = 1.2U$ for attached C). The unit cells of 1 and 2 contain molecules of a disordered solvent (two in 1 and one in 2) whose identity could not be assigned from crystallographic data. ^1H NMR spectra indicate that these disordered solvent molecules are CH_3CN molecules. Full occupancy has been assumed, and the density calculations reflect this assumption. All non-hydrogen atoms of 3 and 4 were refined with anisotropic thermal parameters. In 1 all non-hydrogen and non-carbon atoms were refined with anisotropic thermal parameters and in 2 all non-hydrogen atoms except those of the solvent molecule were refined with anisotropic thermal parameters.

Tables IV–VII contain positional parameters for 1–4, respectively. Tables VIII–XI contain selected bond distances and bond angles for 1–4, respectively.

All computer programs and the sources of the scattering factors are contained in the SHELXTL program library (Version 5.1, G. Sheldrick, Nicolet (Siemens), Madison, WI).

Acknowledgment. This work was supported by grants from the National Science Foundation.

Supplementary Material Available: Tables of positional parameters and isotropic thermal parameters for non-hydrogen atoms (Tables IV–VII), bond lengths, bond angles, anisotropic thermal parameters, and hydrogen atom parameters for 1–4 (35 pages); tables of observed and calculated structure factors for 1–4 (42 pages). Ordering information is given on any current masthead page.